cosmetics

MDPI

Article

Cosmetic Anti-Aging Potential of the Traditional Thai Longevity Formula Mai-Kae-Den-Klong: Mechanistic Insights from Enzyme-Based Bioassays and In Silico Analysis

Theeraphan Chumroenphat [1], Nattapong Wongchum [2], Surapon Saensouk [3], Kusawadee Plekratoke [1], Panupong Mahalapbutr [4], Khin Soe Win [4], Saran Chaweerak [5], Subramani Paranthaman Balasubramani [6] and Ananya Dechakhamphu [1,*]

[1] Cosmetic Science and Spa Program, Faculty of Thai Traditional and Alternative Medicine, Ubon Ratchathani Rajabhat University, Ubonratchathani 34000, Thailand; theeraphan.c@ubru.ac.th (T.C.); kusawadee.p@ubru.ac.th (K.P.)
[2] Biology Program, Faculty of Science, Ubon Ratchathani Rajabhat University, Ubonratchathani 34000, Thailand; nattapong.w@ubru.ac.th
[3] Biodiversity Program, Diversity of Family Zingiberaceae and Vascular Plant for Its Applications Research Unit, Walai Rukhavej Botanical Research Institute, Mahasarakham University, Kantarawichai 44150, Maha Sarakham, Thailand; surapon.s@msu.ac.th
[4] Department of Biochemistry, Faculty of Medicine, Khon Kaen University, Khon Kaen 40002, Thailand; panupma@kku.ac.th (P.M.); khinsoe.w@kkumail.com (K.S.W.)
[5] Thai Traditional Medicine Program, Faculty of Thai Traditional and Alternative Medicine, Ubon Ratchathani Rajabhat University, Ubonratchathani 34000, Thailand; saran.c@ubru.ac.th
[6] Department of Natural Sciences, Albany State University, Albany, GA 31707, USA; balasubramani.subramaniparanthaman@asurams.edu
* Correspondence: ananya.d@ubru.ac.th

Abstract

Skin aging is associated with oxidative stress, extracellular matrix degradation, and dysregulation of melanogenesis, leading to wrinkles, loss of elasticity, and hyperpigmentation. Natural plant-derived compounds have attracted increasing interest as multifunctional cosmetic ingredients due to their antioxidant and anti-aging properties. Mai-Kae-Den-Klong (MKDK), a traditional Thai longevity herbal formula composed of *Albizia procera* (Roxb.) Benth., *Cyperus rotundus* L., *Diospyros rhodocalyx* Kurz, *Piper nigrum* L., *Streblus asper* Lour., and *Tinospora crispa* (L.) Hook.f. & Thomson, has historically been used to promote vitality and healthy aging; however, its potential application as a cosmetic anti-aging ingredient remains scientifically unexplored. Therefore, this study investigated the anti-aging potential of MKDK extract using integrated enzyme-based bioassays and in silico approaches. Phytochemical profiling of the ethanolic extract was performed using LC-MS analysis, revealing diverse bioactive constituents, including flavonoids, phenolic glycosides, alkaloids, and terpenoids, with (−)-epicatechin, procyanidin B1, and piperine identified as major metabolites. Antioxidant activity was evaluated using 2,2-diphenyl-1-picrylhydrazyl (DPPH) and 2,2′-azino-bis(3-ethylbenzothiazoline-6-sulfonic acid) (ABTS) radical scavenging assays, while inhibitory activities against tyrosinase, collagenase, elastase, and hyaluronidase were assessed to determine skin anti-aging potential. The extract exhibited strong antioxidant activity, with IC_{50} values of 17.23 ± 2.11 μg/mL for DPPH and 11.87 ± 1.77 μg/mL for ABTS assays. In addition, the extract demonstrated inhibitory effects against tyrosinase (IC_{50} = 41.25 ± 1.56 μg/mL), elastase (IC_{50} = 49.51 ± 3.69 μg/mL), collagenase (IC_{50} = 61.54 ± 2.88 μg/mL), and hyaluronidase (IC_{50} = 63.74 ± 6.32 μg/mL), suggesting multifunctional anti-aging properties associated with skin brightening and extracellular matrix preservation. Network pharmacology analysis predicted multiple

Check for updates

Received: 9 May 2026
Revised: 10 June 2026
Accepted: 12 June 2026
Published: 18 June 2026

Copyright: © 2026 by the authors. Licensee MDPI, Basel, Switzerland. This article is an open access article distributed under the terms and conditions of the Creative Commons Attribution (CC BY) license.

aging-related signaling pathways, particularly the FoxO signaling pathway, which is associated with oxidative stress regulation and longevity. Molecular docking analysis further demonstrated favorable binding affinities of procyanidin B1, epicatechin, and piperine toward skin-aging-related enzymes, supporting their potential contribution to the observed bioactivities. Overall, these findings suggest that MKDK possesses promising cosmeceutical potential as a natural multifunctional anti-aging ingredient and provides scientific support for the application of traditional Thai herbal formulations in cosmetic and skin health products.

Keywords: skin aging; polyherbal extract; cosmeceutical potential; phytochemicals; traditional Thai medicine; enzyme inhibition

1. Introduction

Skin aging is a complex and progressive biological process driven by the interaction of intrinsic factors, including genetics and hormonal changes, and extrinsic factors such as ultraviolet (UV) radiation, environmental pollution, smoking, and dietary habits [1,2]. These cumulative factors contribute to structural and functional deterioration of the skin, leading to visible manifestations including wrinkles, loss of elasticity, dryness, roughness, and hyperpigmentation [3]. At the molecular level, skin aging is closely associated with oxidative stress, chronic inflammation, and degradation of the extracellular matrix (ECM), processes largely mediated by the excessive production of reactive oxygen species (ROS). Elevated ROS levels stimulate the activity of matrix-degrading enzymes, including collagenase, elastase, and hyaluronidase, resulting in the breakdown of collagen, elastin, and hyaluronic acid, which are essential components responsible for skin firmness, elasticity, and hydration [1,4]. In addition, increased tyrosinase activity contributes to abnormal melanogenesis and age-related pigmentation disorders [5]. Owing to the growing consumer demand for healthy and youthful skin, considerable attention has been directed toward the development of safe, effective, and naturally derived multifunctional anti-aging agents [6].

Natural products and plant-derived bioactive compounds have emerged as promising candidates for cosmetic and dermatological applications due to their diverse pharmacological properties, particularly antioxidant, anti-inflammatory, and enzyme-inhibitory activities [7,8]. Phytochemicals such as flavonoids, tannins, and alkaloids have demonstrated strong ROS-scavenging capacity and the ability to inhibit ECM-degrading enzymes, thereby protecting skin structural integrity and delaying aging-related deterioration [9]. Compared with synthetic cosmetic ingredients, plant-derived compounds are increasingly investigated as cosmetic ingredients due to their diverse biological activities and long history of traditional use [10]. Consequently, traditional herbal medicines have gained increasing scientific interest as potential sources of functional cosmeceutical ingredients capable of promoting dermal regeneration, preserving ECM homeostasis, and improving skin appearance [11–15]. These findings support the expanding application of medicinal plants in the development of natural anti-aging cosmetic formulations [16].

In Thai traditional medicine, Mai-Kae-Den-Klong (MKDK) is recognized as a traditional oral longevity formula composed of six medicinal plants: *Albizia procera* (Roxb.) Benth. (White Siris), *Cyperus rotundus* L. (Nutgrass), *Diospyros rhodocalyx* Kurz (Tako), *Piper nigrum* L. (Black pepper), *Streblus asper* Lour. (Khoi), and *Tinospora crispa* (L.) Hook.f. & Thomson (Petawali). Several individual components of this formulation have been reported to possess biological activities relevant to anti-aging and skin health. *A. procera* exhibits potent antioxidant activity [17,18], while *C. rotundus* has been shown to improve longevity

and metabolic regulation in a *Drosophila melanogaster* model under high-fat diet conditions [19,20]. *D. rhodocalyx* demonstrates antioxidant, antibacterial, and anti-inflammatory properties [21–25]. Piperine, the major alkaloid of *P. nigrum*, has been widely investigated for its antioxidant, anti-inflammatory, and pharmacological activities [26]. Furthermore, *S. asper* and *T. crispa* have been associated with anti-aging, neuroprotective, and anti-diabetic effects [27–29]. Although these medicinal plants individually exhibit promising bioactivities, scientific evidence regarding the complete MKDK polyherbal formulation remains limited. Importantly, traditional Thai herbal formulations are conceptually designed based on combinations of multiple herbs that may provide complementary biological activities and therapeutic benefits while minimizing toxicity, highlighting the need for comprehensive scientific validation of their biological functions and mechanisms of action.

Therefore, the present study aimed to evaluate the cosmetic anti-aging potential of MKDK and investigate the phytochemical constituents and possible molecular mechanisms associated with its bioactivity. This work was conducted to provide scientific evidence supporting the traditional use of MKDK and to explore its potential as a source of natural bioactive ingredients for cosmetic applications [30–33]. Furthermore, the study contributes to bridging traditional Thai medicinal knowledge with contemporary pharmacological research and may facilitate the development of plant-derived anti-aging cosmeceutical products [34–36].

2. Materials and Methods

2.1. Plant Materials and Preparation of Plant Extracts

Albizia procera (bark), *Cyperus rotundus* (tuber and rhizome), *Diospyros rhodocalyx* (bark), *Piper nigrum* (seed), *Streblus asper* (seed), and *Tinospora crispa* (stem) were collected from local cultivation farms in Ubon Ratchathani Province, Thailand, where they are traditionally grown for medicinal and general purposes. All plant materials were thoroughly washed with tap water and air-dried, followed by oven drying at 55 °C using a hot air oven (Memmert GmbH + Co. KG, Schwabach, Germany). Each dried plant material was then ground into a fine powder. Equal quantities (100 g) of each powdered herb were accurately weighed and combined. The mixed powder was extracted by maceration with 1500 mL of 80% ethanol (Merck KGaA, Darmstadt, Germany) at room temperature for 3 days with continuous agitation. After maceration, the extract was filtered to obtain the ethanolic fraction. The plant residue was subjected to a second round of extraction using an additional 1500 mL of 80% ethanol under the same conditions. Following the second maceration period, the mixture was again filtered. The ethanolic filtrates from both extraction rounds were combined and concentrated under reduced pressure using a rotary evaporator at 55 °C to remove the solvent. The resulting concentrate was then lyophilized using a freeze dryer (LaboGene ApS, Lynge, Denmark). The final dried extract was stored at 4 °C until further analysis. This extraction method was selected based on preliminary screening, which indicated that it yielded the highest antioxidant activity among the different conditions tested.

2.2. LC-MS Analysis of Formula Extract

Approximately 20.0 mg of dried extract was accurately weighed and dissolved in 80% ethanol. The solution contained sulfadimethoxine (Sigma-Aldrich, St. Louis, MO, USA) at a final concentration of 25 ng/mL as an internal standard. The samples were vortexed thoroughly and then centrifuged at 14,000 rpm for 10 min. The resulting supernatants were carefully transferred to LC-MS vials and subjected to liquid chromatography-mass spectrometry (LC-MS) analysis [37].

The LC separation was performed using a Poroshell 120 EC-C18 column (2.1 × 100 mm, 2.7 μm particle size) maintained at 50 °C. The injection volume was 10 μL, and the flow rate was set at 0.4 mL/min. The mobile phases consisted of 0.1% formic acid (Sigma-Aldrich, St. Louis, MO, USA) in water (solvent A) and 0.1% formic acid in acetonitrile (Sigma-Aldrich, St. Louis, MO, USA) (solvent B). The gradient elution program was as follows: 0–0.5 min, 100% A; 0.5–10.5 min, linear gradient to 55% B; 10.5–12.5 min, linear gradient to 75% B; 12.5–14.0 min, linear gradient to 100% B; 14.0–17.0 min, held at 100% B; 17.0–17.5 min, returned to 100% A; and 17.5–20.0 min, re-equilibrated at 100% A.

Mass spectrometric detection was carried out on an Agilent 6545XT LC-QTOF mass spectrometer (Agilent Technologies, Santa Clara, CA, USA) operated in both positive and negative electrospray ionization (ESI) modes under high-resolution conditions. The drying gas temperature was set at 325 °C with a gas flow of 13 L/min, while the sheath gas temperature was 275 °C with a flow of 12 L/min. The nebulizer pressure was 45 psi. The capillary voltage was set at +4000 V for positive mode and −3000 V for negative mode. The MS1 scan range was set from m/z 40 to 1700, and the MS2 scan range was from m/z 25 to 1000. Collision energy was set at 20 eV for positive ion mode and 10 eV for negative ion mode. The data acquisition rate was 3.35 spectra per second, allowing up to 10 precursors per cycle with a minimum intensity threshold of 5000 counts and a retention time threshold of 0.001%. Reference masses were used for real-time mass axis correction: m/z 121.0509 and 922.0098 in positive mode, and m/z 112.9856 and 1033.9881 in negative mode.

Data processing was carried out using MS-Dial version 5.3. Normalization was carried out using sulfadimethoxine as an internal standard. Specific reference masses were excluded from analysis, including m/z 121.0509 and 922.0098 in positive mode, and m/z 112.9856, 119.0363, 966.0007, and 1033.9881 in negative mode. Ion adducts considered were $[M + H]^+$ for positive mode and $[M - H]^-$ for negative mode. Compound identification was conducted using MS-Dial's in-house ESI (+/−) MS/MS library from authentic standards, along with external databases including the Fiehn/Vaniya Natural Products Library and the BMDMS-NP database. Metabolite annotation based on LC-MS/MS spectral matching was considered putative identification according to the Metabolomics Standards Initiative (MSI) guidelines (Level 2), as compound identities were not confirmed using authentic reference standards. Data pre-filtration criteria included a retention time range of 0.2–18 min, a signal-to-noise ratio (S/N) of ≥5, a peak intensity threshold of >10,000, and an identification score of ≥1.0.

2.3. Gene Ontology (GO) Functional Enrichment Analysis

To investigate the biological processes associated with the anti-aging effects of the longevity formula, a network pharmacology approach was employed. Based on the SMILES structures of key phytochemicals, a total of 101 target genes were identified and annotated through GO enrichment analysis. Only targets with a prediction probability score (P) equal to 1 were selected to ensure high-confidence target identification. This analysis was conducted to substantiate the traditional use of the formula in promoting anti-aging. The SMILES representations of the principal compounds in the longevity formula were submitted to the SwissTargetPrediction database to predict potential protein targets [38]. Protein–protein interaction (PPI) networks were generated using Homo sapiens as the reference organism, applying a high confidence score threshold (>0.9). The biological roles of the identified targets were further classified and interpreted through GO enrichment analysis using ShinyGO 0.80 [39–41], providing insight into the potential molecular mechanisms underlying the longevity-promoting effects of the formula.

2.4. 2,2-Diphenyl-1-Picrylhydrazyl (DPPH) Free Radical Scavenging Assay

The antioxidant activity of the longevity formula extract was assessed using the DPPH assay. A mixture of 180 µL extract and 20 µL of 1 mM DPPH (Sigma-Aldrich, St. Louis, MO, USA) prepared in methanol was incubated in the dark at room temperature for 30 min. Absorbance was measured at 517 nm using a microplate reader (Biochrom Ltd., Cambridge, UK). Each sample was analyzed in triplicate. The percentage of inhibition was calculated as:

$$\text{Inhibition (\%)} = [(\text{OD_control} - \text{OD_sample})/\text{OD_control}] \times 100 \quad (1)$$

The IC_{50} value was determined from a linear regression of inhibition percentages at extract concentrations ranging from 0–500 µg/mL (diluted in sterile water) [37].

2.5. 2,2′-Azino-Bis(3-Ethylbenzothiazoline-6-Sulfonic Acid) (ABTS) Free Radical Scavenging Assay

For the ABTS assay, 20 µL of the extract was mixed with 180 µL of $ABTS^{\bullet}$ solution (prepared from 7 mM ABTS and 2.45 mM ammonium persulfate (Sigma-Aldrich, St. Louis, MO, USA), incubated 12–16 h in the dark, and adjusted to an absorbance of ~0.700 at 734 nm). After 10 min of incubation in the dark, absorbance was read at 734 nm. Inhibition was calculated using the same formula as above. IC_{50} values were determined from inhibition curves across concentrations of 0–500 µg/mL [42].

2.6. Anti-Collagenase Activity Assay

The inhibitory activity of the longevity formula extract against collagenase was evaluated following the method of Angelis et al. [43] with minor modifications. Tris-HCl buffer (10 mM, pH 7.3) was prepared by dissolving Tris(hydroxymethyl)aminomethane (Tris base; Sigma-Aldrich, St. Louis, MO, USA) in deionized water and adjusting the pH to 7.3 with hydrochloric acid (HCl; Merck, Darmstadt, Germany). Collagenase from *Clostridium histolyticum* (Sigma-Aldrich, St. Louis, MO, USA) was dissolved in Tris-HCl buffer to obtain a final concentration of 0.1 U/mL. The substrate N-[3-(2-furyl)acryloyl]-Leu-Gly-Pro-Ala (FALGPA; Sigma-Aldrich, St. Louis, MO, USA) was prepared at a concentration of 0.8 mM in Tris-HCl buffer immediately before use. Briefly, 25 µL of Tris-HCl buffer was added to each well of a 96-well microplate, followed by 25 µL of the test sample and 25 µL of collagenase enzyme solution. The reaction mixtures were incubated at 37 °C for 15 min in the dark. Subsequently, 25 µL of FALGPA solution was added, and the mixtures were incubated for an additional 30 min at 37 °C under light-protected conditions. Absorbance was measured at 345 nm using a microplate reader. Each sample was tested in triplicate. Oleanolic acid (Sigma-Aldrich, St. Louis, MO, USA) at a concentration of 1 mg/mL was used as the positive control. The percentage of collagenase inhibition was calculated using the following formula:

$$\text{Inhibition (\%)} = [(\text{OD_control} - \text{OD_sample})/\text{OD_control}] \times 100 \quad (2)$$

2.7. Anti-Elastase Activity Assay

The inhibitory effect of the longevity formula extract on elastase activity was determined based on the method described by Lee et al. [44] with slight modifications. Elastase from porcine pancreas (Sigma-Aldrich, St. Louis, MO, USA) was dissolved in 0.2 M Tris-HCl buffer (pH 8.0) to obtain a final concentration of 7.5 U/mL. The substrate N-succinyl-Ala-Ala-Pro-p-nitroanilide (SANA; Sigma-Aldrich, St. Louis, MO, USA) was prepared at a concentration of 0.8 mM in methanol immediately before use. In each well of a 96-well plate, 160 µL of Tris-HCl buffer was added, followed by 20 µL of the test sample and 20 µL of elastase enzyme solution. The mixture was incubated at 25 °C for 20 min. Then, 20 µL

of SANA solution was added to initiate the reaction. The plate was incubated again at 25 °C for 20 min under light-protected conditions. The absorbance was measured at 410 nm using a microplate reader. All measurements were performed in triplicate. Oleanolic acid (1 mg/mL) was used as a positive control. The percentage of elastase inhibition was calculated using the following formula:

$$\text{Inhibition (\%)} = [(\text{OD_control} - \text{OD_sample})/\text{OD_control}] \times 100 \quad (3)$$

2.8. Anti-Hyaluronidase Activity Assay

The hyaluronidase inhibitory activity of the longevity formula extract was assessed according to the method of Abdelfattah et al. [45] with slight modifications. Hyaluronidase from bovine testes (Sigma-Aldrich, St. Louis, MO, USA) was prepared at a concentration of 1.5 mg/mL in 300 mM phosphate buffer (pH 5.35). Hyaluronic acid (Sigma-Aldrich, St. Louis, MO, USA) was prepared at a concentration of 100 mg/mL in 0.1 M acetate buffer (pH 3.5). The reaction mixture consisted of 25 µL of the test sample, 25 µL of hyaluronidase enzyme solution (1.5 mg/mL), and 25 µL of 300 mM phosphate buffer (pH 5.35). The mixture was incubated at 37 °C for 15 min. Subsequently, 100 µL of hyaluronic acid substrate (100 mg/mL in 0.1 M acetate buffer, pH 3.5) was added, and the mixture was incubated again at 37 °C for 45 min. To stop the reaction, 100 µL of acidic albumin solution—containing 79 mM acetic acid, 24 mM sodium acetate, and 1% (*w*/*v*) bovine serum albumin—was added, followed by a final incubation at room temperature for 30 min. The absorbance was measured at 600 nm using a microplate reader. Each sample was tested in triplicate. Oleanolic acid (1 mg/mL) was used as a positive control. The percentage inhibition of hyaluronidase activity was calculated using the following equation:

$$\text{Inhibition (\%)} = [(\text{OD_control} - \text{OD_sample})/\text{OD_control}] \times 100 \quad (4)$$

2.9. Anti-Tyrosinase Activity Assay

Tyrosinase inhibition was assessed using a 50 mM phosphate buffer (pH 6.5) prepared from potassium dihydrogen phosphate (KH_2PO_4; Sigma-Aldrich, St. Louis, MO, USA). L-Tyrosine (Sigma-Aldrich, St. Louis, MO, USA) was prepared at a concentration of 2 mM in the same buffer, while tyrosinase from mushroom (Sigma-Aldrich, St. Louis, MO, USA) was prepared at a concentration of 167 U/mL. Test samples were dissolved in dimethyl sulfoxide (DMSO). The reaction mixture contained 70 µL of sample, 110 µL of L-tyrosine, and 30 µL of tyrosinase, and was incubated at room temperature for 30 min. Absorbance was measured at 492 nm, and enzyme inhibition was calculated as:

$$\text{Inhibition (\%)} = [(\text{OD_control} - \text{OD_sample})/\text{OD_control}] \times 100 \quad (5)$$

2.10. Molecular Docking Analysis

The three-dimensional structures of the selected phytochemicals, including alpha-cyperone (CID: 6452086), D-tetrahydropalmatine (CID: 969488), epicatechin (CID: 72276), piperine (CID: 638024), and procyanidin B1 (CID: 11250133), were obtained from the PubChem database (https://pubchem.ncbi.nlm.nih.gov/) in Structure Data File (SDF) format. To ensure appropriate ionization states under physiological conditions, protonation of each compound at pH 7.4 was evaluated and optimized using MarvinSketch software V24.1.3 (ChemAxon, Budapest, Hungary). The prepared ligand structures were subsequently used for molecular docking analysis.

The crystal structures of skin-aging-related target enzymes, including tyrosinase (PDB ID: 2Y9X), elastase (PDB ID: 1BRU), collagenase (PDB ID: 2Y6I), and hyaluronidase (PDB ID: 2PE4), were retrieved from the Protein Data Bank (PDB; https://www.rcsb.

org/). These enzymes were selected due to their important roles in melanogenesis and extracellular matrix degradation associated with skin aging. Prior to docking analysis, protein structures were prepared by removing water molecules and non-essential co-crystallized ligands. Molecular docking simulations were performed using the CB-Dock2 web server, an automated cavity-detection docking platform based on AutoDock Vina v1.2.5 algorithms. The docking procedure predicted the optimal binding conformations and binding affinities between the selected phytochemicals and target proteins within the active-site regions.

The binding interactions between ligands and target proteins were further analyzed and visualized using BIOVIA Discovery Studio Visualizer (Dassault Systèmes BIOVIA, San Diego, CA, USA). The interaction analysis included hydrogen bonding, hydrophobic interactions, π–π stacking, van der Waals interactions, and interactions with catalytic amino acid residues and metal ions located within the active sites of the enzymes. The docking scores were expressed as binding energies (kcal/mol), where lower binding energy values indicate stronger predicted binding affinity and greater interaction stability between the phytochemicals and the target enzymes.

2.11. Statistical Analysis

Data are presented as mean ± standard deviation (SD). Student's *t* test was employed for comparison of means. Statistical analyses were conducted using SPSS version 20.0, and graphical representations were generated using SigmaPlot version 10.0. A *p*-value of less than 0.05 was considered statistically significant. No adjustment for multiple comparisons was applied because the analyses were exploratory and involved predefined comparisons.

3. Results

3.1. Phytochemical Profiles of MKDK Formula Extract

LC-MS analysis of the MKDK extract revealed a diverse metabolite profile, comprising a wide range of phytochemicals associated with antioxidant, anti-inflammatory, and skin-beneficial properties. A total 2186 compounds were detected, spanning various chemical classes including flavonoids, alkaloids, terpenoids, lignans, and fatty acid derivatives. Among them, (−)-epicatechin showed the highest peak intensity, followed by procyanidin B1, piperine, D-tetrahydropalmatine (rotundine), and alpha-cyperone. These compounds are well-recognized for their antioxidant and anti-aging activities. The presence of alpha-cyperone and other sesquiterpenoids indicates possible contributions from *C. rotundus*. Additionally, phenolic glycosides, lignan glycosides, and coumarin derivatives were identified, which may contribute to the overall bioactivity of the extract. The broad chemical diversity and high abundance of bioactive metabolites support the potential of MKDK as a multi-targeted formula for skin anti-aging applications. The top 50 selected compounds are presented in Table 1, while the full list of identified metabolites is provided in Supplementary Table S1.

Table 1. Selected metabolites identified in the MKDK extract by LC-MS analysis, based on peak intensity.

No.	Metabolite Name	RT (min)	*m/z*	Adduct Type	Ontology	Total Score	Peak Intensity
1	(−)-Epicatechin	3.740	289.08139	$[M-H]^-$	Catechins	1.39	129,940,398.08
2	Procyanidin B1	3.523	577.14099	$[M-H]^-$	Biflavonoids and polyflavonoids	1.42	72,402,025.91
3	Piperine	10.327	308.13287	$[M+Na]^+$	Morphinans	1.00	67,279,924.56
4	D-Tetrahydropalmatine (rotundine)	4.940	356.18518	$[M+H]^+$	Protoberberine alkaloids and derivatives	1.14	52,947,476.27
5	Alpha-cyperone (essential oils of *Cyperus rotundus* (nutgrass))	11.993	219.18153	$[M+H]^+$	Eudesmane, isoeudesmane, or cycloeudesmane sesquiterpenoids	1.43	50,673,704.22

Table 1. *Cont.*

No.	Metabolite Name	RT (min)	*m/z*	Adduct Type	Ontology	Total Score	Peak Intensity
6	4-Hydroxy-5-[(2S,3R,4S,5S,6R)-3,4,5-trihydroxy-6-(hydroxymethyl)oxan-2-yl]oxy-1H-benzo[f][2]benzofuran-3-one	0.692	377.08560	$[M-H]^-$	Phenolic glycosides	1.12	47,944,579.66
7	Feruloyltyramine	6.251	314.14206	$[M+H]^+$	Hydroxycinnamic acids and derivatives	1.58	44,707,331.76
8	Tetrahydropalmatin	0.807	356.18918	$[M+H]^+$	Protoberberine alkaloids and derivatives	1.23	39,378,926.05
9	9-HODE	12.613	295.23352	$[M-H]^-$	Lineolic acids and derivatives	1.50	38,647,009.98
10	N6-Isopentenyladenosine	11.325	336.16376	$[M+H]^+$	Purine nucleosides	1.17	38,239,568.75
11	Methyl3-[3,4-dihydroxy-5-(3-methylbut-2-enyl)phenyl]-2-[[4-hydroxy-3-(3-methylbut-2-enyl)phenyl]methyl]-4-methoxy-5-oxofuran-2-carboxylate	6.129	521.20874	$[M-H]^-$	Catechols	1.04	34,453,130.32
12	Feruloyltyramine	6.631	312.13370	$[M-H]^-$	Hydroxycinnamic acids and derivatives	1.15	33,778,398.78
13	Leonurine	11.637	334.14691	$[M+Na]^+$	Gallic acid and derivatives	1.00	32,791,351.74
14	Piperazine-2,5-dione	10.394	115.05392	$[M+H]^+$	Alpha amino acids and derivatives	1.28	32,602,446.83
15	Betaine	0.869	118.08587	$[M+H]^+$	Alpha amino acids	1.31	32,272,155.30
16	Piperanine	10.182	288.16806	$[M+H]^+$	Benzodioxoles	1.50	30,142,204.97
17	FA 18:1 + 2O	11.299	313.23984	$[M-H]^-$	Long-chain fatty acids	1.38	29,478,221.72
18	2-[(1S,2S,4aR,8aS)-1-Hydroxy-4a-methyl-8-methylidene-1,2,3,4,5,6,7,8a-octahydronaphthalen-2-yl]prop-2-enoic acid	10.207	249.15112	$[M-H]^-$	Eudesmane, isoeudesmane or cycloeudesmane sesquiterpenoids	1.33	28,438,014.32
19	Ganoderic acid	12.000	593.26825	$[M+Na]^+$	Triterpenoids	1.47	28,106,746.55
20	Tetrandrine	13.287	623.31061	$[M+H]^+$	Lignans, neolignans and related compounds	1.03	26,602,906.87
21	Procyanidin C1	3.814	865.19739	$[M-H]^-$	Biflavonoids and polyflavonoids	1.15	26,537,928.13
22	Lathyrol	5.780	357.19254	$[M+Na]^+$	Diterpenoids	1.16	25,678,670.35
23	Apiin	4.721	563.14069	$[M-H]^-$	Flavonoid-7-O-glycosides	1.44	24,681,475.27
24	2-[[7-Hydroxy-1-(4-hydroxy-3,5-dimethoxyphenyl)-3-(hydroxymethyl)-6,8-dimethoxy-1,2,3,4-tetrahydronaphthalen-2-yl]methoxy]oxane-3,4,5-triol	5.743	587.19080	$[M+Cl]^-$	Lignan glycosides	1.18	24,611,829.07
25	Arctiin	8.180	579.21008	$[M+HCOO]^-$	Lignan glycosides	1.03	23,253,699.11
26	Trehalose	0.969	341.10880	$[M-H]^-$	O-glycosyl compounds	1.21	21,538,659.87
27	Hetisine	12.347	352.19061	$[M+Na]^+$	Atisane diterpenoids	1.22	21,288,368.25
28	NCGC00385831-01!7-Hydroxy-3-(2-methylbut-3-en-2-yl)-6-(3-methylbut-2-enyl)chromen-2-one	11.914	316.19720	$[M+NH_4]^+$	7-hydroxycoumarins	1.14	21,235,583.31
29	Dehydrosalsolidine	5.820	206.11842	$[M+H]^+$	Dihydroisoquinolines	1.49	20,881,987.08
30	Kaempferol	6.853	285.04263	$[M-H]^-$	Flavonols	1.48	20,321,696.02
31	N-(1-((2-Amino-2-oxoethyl)amino)-4-methyl-1-oxopentan-2-yl)-1-(8-(6,7-dimethyl-4-oxo-4H-chromen-2-yl)-4H-benzo[d][1,3]dioxine-6-carbonyl)pyrrolidine-2-carboxamide	12.809	619.27802	$[M+H]^+$	Oligopeptides	1.07	20,107,860.93
32	NCGC00385817-01!(2E,4E)-N-(2-Methylpropyl)deca-2,4-dienamide	12.147	224.20242	$[M+H]^+$	N-acyl amines	1.30	19,846,242.05
33	14-Hydroxy-3-((5-hydroxy-4-methoxy-6-methyltetrahydro-2H-pyran-2-yl)oxy)-10,13-dimethyl-17-(5-oxo-2,5-dihydrofuran-3-yl)hexadecahydro-1H-cyclopenta[a]phenanthren-16-yl acetate	13.454	599.31561	$[M+Na]^+$	Cardenolide glycosides and derivatives	1.31	19,804,425.09
34	Mundulone	5.319	433.17163	$[M-H]^-$	6-prenylated isoflavanones	1.03	19,589,207.50
35	16-Hydroxyhexadecanoic acid	14.188	271.22931	$[M-H]^-$	Long-chain fatty acids	1.20	19,364,700.28
36	FA 18:2 + 3O	8.045	327.22092	$[M-H]^-$	Lineolic acids and derivatives	1.42	17,407,509.12
37	trans-Ferulic acid; $[M+H-H_2O]+$; CE30; KSEBMYQBYZTDHS-HWKANZROSA-N	6.633	177.05449	$[M+H-H_2O]^+$	Hydroxycinnamic acids	1.39	16,377,095.92
38	(2S,3S)-2-(3,4,5-Trihydroxyphenyl)-3,4-dihydro-2H-chromene-3,5,7-triol	2.914	305.06680	$[M-H]^-$	Epigallocatechins	1.45	15,398,610.02

Table 1. *Cont.*

No.	Metabolite Name	RT (min)	*m/z*	Adduct Type	Ontology	Total Score	Peak Intensity
39	13-HOTrE	12.014	293.21246	[M − H]1$^-$	Lineolic acids and derivatives	1.34	15,131,678.43
40	2-[(2S,4aR,8aS)-2-Hydroxy-4a-methyl-8-methylidene-3,4,5,6,7,8a-hexahydro-1H-naphthalen-2-yl]prop-2-enoic acid	9.396	249.14955	[M − H]$^-$	Eudesmane, isoeudesmane or cycloeudesmane sesquiterpenoids	1.31	14,680,215.15
41	Tiliroside	2.903	593.12964	[M − H]$^-$	Flavonoid 3-O-p-coumaroyl glycosides	1.12	13,963,657.20
42	FA 18:2 + O	12.956	293.21252	[M − H]$^-$	Long-chain fatty acids	1.34	13,437,213.35
43	Choline; CE10; OEYIOHPDSNJKLS-UHFFFAOYSA-N	0.667	104.10968	[M]$^+$	Cholines	1.36	13,260,052.05
44	Syringin	3.911	395.13126	[M + Na]$^+$	Phenolic glycosides	1.34	13,110,436.45
45	FA 18:3 + 2O	10.262	309.20734	[M − H]$^-$	Medium-chain fatty acids	1.29	13,028,882.42
46	(Z)-5,8,11-Trihydroxyoctadec-9-enoic acid	8.530	353.22897	[M + Na]$^+$	Long-chain fatty acids	1.04	12,942,499.65
47	4′-O-(2′-E-Coumaroyl GluA)(1-2)GluA) Apigenin	7.562	269.04553	[M − H]$^-$	Flavonoid O-glucuronides	1.27	12,889,406.22
48	Phytosphingosine	11.361	318.30099	[M + H]$^+$	1,3-aminoalcohols	1.45	12,559,947.59
49	4-Hydroxy-2′,4′,6′-trimethoxychalcone	6.896	313.10806	[M − H]$^-$	Cinnamylphenols	1.34	12,464,761.57
50	Catechin	3.722	291.08585	[M + H]$^+$	Catechins	1.22	11,609,961.08

3.2. GO Functional Enrichment Analysis

Network pharmacology analysis identified several key biological pathways potentially modulated by the phytochemicals in the MKDK formula. KEGG enrichment highlighted the top enriched pathways, which included metabolism, lipid and atherosclerosis, viral carcinogenesis, focal adhesion, and chemokine signaling, with significant fold enrichment and false discovery rates (FDRs). Among them, FoxO signaling is particularly relevant to aging, as it plays a central role in cellular oxidative stress response, apoptosis regulation, and longevity. Additionally, pathways related to immune modulation (e.g., chemokine and Fc epsilon RI signaling), cell junction integrity, and endocrine resistance suggest multi-system anti-aging activity (Figure 1). These results further substantiate the multi-target, multi-pathway nature of the formula and align with its observed antioxidant and anti-aging enzyme activities.

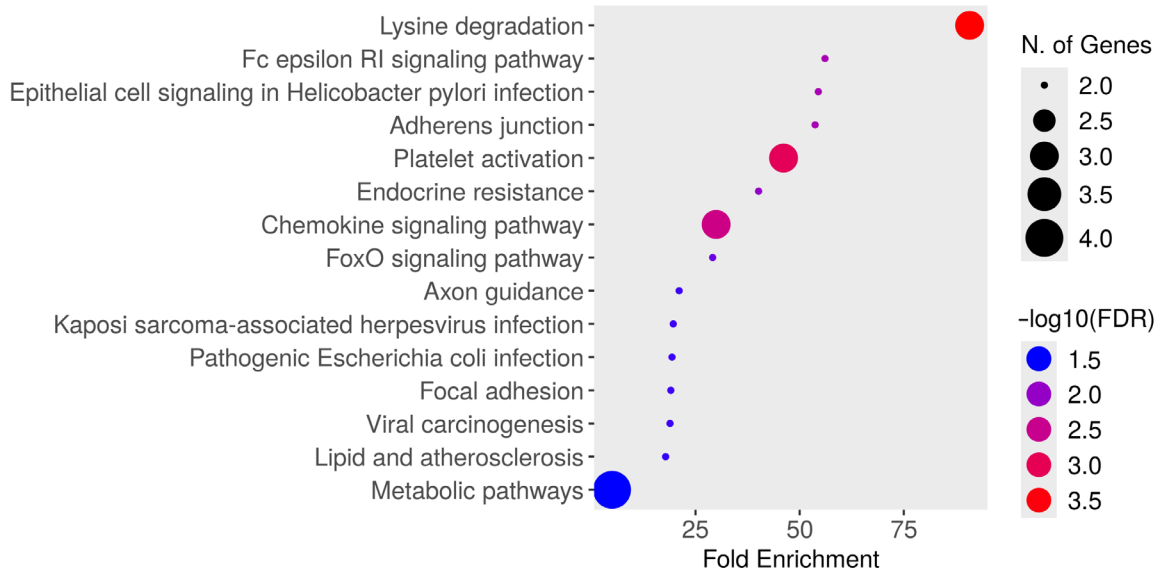


Figure 1. Kyoto Encyclopedia of Genes and Genomes (KEGG) pathway enrichment analysis of predicted target genes associated with phytochemicals from the MKDK formula. The *x*-axis represents fold enrichment. Bubble size indicates the number of genes associated with each pathway, and bubble color represents statistical significance expressed as the negative logarithm of the false discovery rate ($-\log_{10}$ FDR).

3.3. Antioxidant Activity of MKDK Extract

The antioxidant capacity of the MKDK formula extract was evaluated using DPPH and ABTS radical scavenging assays (Table 2). The extract exhibited dose-dependent antioxidant activity, with IC_{50} values of 17.23 ± 2.11 μg/mL and 11.87 ± 1.77 μg/mL in the DPPH and ABTS assays, respectively. Although less potent than the reference antioxidant α-tocopherol (IC_{50} = 4.25 ± 0.15 μg/mL for DPPH and 3.04 ± 0.08 μg/mL for ABTS), the formula demonstrated significant free radical scavenging potential. These findings suggest that the polyherbal extract possesses strong antioxidant activity, which may contribute to its anti-aging effects by mitigating oxidative stress.

Table 2. Free radical scavenging activities of MKDK formula extract.

Extract/Compounds	IC_{50} (μg/mL)	
	DPPH Assay	**ABTS Assay**
MKDK formula	17.23 ± 2.11 **	11.87 ± 1.77 **
α-Tocopherol	4.25 ± 0.15	3.04 ± 0.08

Data are expressed as mean ± SD (n = 3). ** indicates a statistically significant difference compared to α-tocopherol ($p < 0.01$), as determined by the Student's t-test.

3.4. Inhibition of Skin-Aging-Related Enzymes by MKDK Extract

The MKDK extract exhibited moderate inhibitory effects against enzymes associated with skin aging, including elastase, collagenase, hyaluronidase, and tyrosinase (Table 3). The IC_{50} values were 49.51 ± 3.69 μg/mL for elastase, 61.54 ± 2.88 μg/mL for collagenase, 63.74 ± 6.32 μg/mL for hyaluronidase, and 41.25 ± 1.56 μg/mL for tyrosinase. Compared to the positive control oleanolic acid, which exhibited stronger inhibition (e.g., elastase IC_{50} = 18.21 ± 2.37 μg/mL), the formula demonstrated significant but lower potency. For tyrosinase inhibition, the extract was less potent than kojic acid (IC_{50} = 23.05 ± 0.92 μg/mL). These findings suggest that MKDK possesses multi-targeted enzyme inhibitory activity, which may contribute to its anti-wrinkle and skin-brightening effects.

Table 3. Enzyme inhibitory activities related to skin aging.

Extract/Compounds	IC_{50} (μg/mL)			
	Elastase	**Collagenase**	**Hyaluronidase**	**Tyrosinase**
MKDK formula	49.51 ± 3.69 **	61.54 ± 2.88 **	63.74 ± 6.32	41.25 ± 1.56 **
Oleanolic acid (positive control)	18.21 ± 2.37	27.56 ± 2.65	57.28 ± 3.14	-
Kojic acid (positive control)	-	-	-	23.05 ± 0.92

Data are expressed as mean ± SD (n = 3). ** indicates a statistically significant difference compared to the respective positive control ($p < 0.01$).

3.5. Molecular Docking Analysis of Key Bioactive Compounds

Molecular docking analysis was performed to predict the binding affinities of key bioactive compounds from the MKDK extract with skin-aging-related enzymes, including tyrosinase, elastase, collagenase, and hyaluronidase (Table 4). Among the tested compounds, procyanidin B1 exhibited the strongest binding affinities toward tyrosinase, elastase, and collagenase, with docking energies of −7.6, −7.7, and −7.7 kcal/mol, respectively. In contrast, piperine demonstrated the highest predicted affinity for hyaluronidase, with a docking score of −7.9 kcal/mol. Epicatechin also showed favorable interactions with the target enzymes, with docking scores ranging from −6.6 to −7.3 kcal/mol. D-tetrahydropalmatine and alpha-cyperone showed relatively weaker but still favorable interactions, particularly with hyaluronidase (−7.2 and −6.5 kcal/mol, respectively). These

in silico findings support the multi-targeted inhibitory potential of the extract and align with the observed in vitro enzyme inhibition results, suggesting that the identified phytochemicals may collectively contribute to the anti-aging activities of the formula.

Table 4. Molecular docking scores (kcal/mol) of selected phytochemicals from the MKDK extract against key skin-aging-related enzymes.

Parameters	Tyrosinase (2Y9X)	Elastase (1BRU)	Collagenase (2Y6I)	Hyaluronidase (2PE4)
Alpha-cyperone ($C_{15}H_{22}O$)	−6.7	−5.1	−5.8	−6.5
D-Tetrahydropalmatine ($C_{21}H_{25}NO_4$)	−6.7	−6.3	−6.6	−7.2
Epicatechin ($C_{15}H_{14}O_6$)	−6.7	−7.3	−6.6	−6.9
Piperine ($C_{17}H_{19}NO_3$)	−6.7	−6.6	−6.7	−7.9
Procyanidin B1 ($C_{30}H_{26}O_{12}$)	−7.6	−7.7	−7.7	−8.2

As shown in Figure 2, molecular docking visualizations revealed that all the selected compounds from the MKDK formula could bind to the active site of tyrosinase (Figure 2a), forming stabilizing interactions with key residues, catalytic histidines, and copper atoms (CuA and CuB). Alpha-cyperone (Figure 2b) and piperine (Figure 2e) were mostly stabilized by van der Waals and alkyl interactions with active-site residues such as HIS85, HIS263, HIS244, PHE264, and MET280, contributing to a binding energy of −6.7 kcal/mol. D-tetrahydropalmatine (Figure 2c) showed a similar binding energy of −6.7 kcal/mol, forming multiple π interactions with key residues. In addition, its aromatic moiety was found to form π–cation interaction with ARG268. Epicatechin (Figure 2d) formed hydrogen bonds with HIS85 and GLU322, maintaining a binding energy of −6.7 kcal/mol. Procyanidin B1 (Figure 2f), which exhibited the strongest binding affinity (−7.6 kcal/mol), formed multiple hydrogen bonds with ASN81, HIS244, ASN260, and GLY281, in addition to extensive van der Waals interactions that further stabilized its orientation within the active-site pocket. Collectively, the visualized interactions support the role of these phytochemicals in tyrosinase inhibition and reinforce their contribution to the anti-pigmentation and anti-aging potential of the formula.

Figure 3 shows the binding interactions between the selected phytochemicals from the MKDK formula and elastase. Alpha-cyperone (Figure 3b) and D-tetrahydropalmatine (Figure 3c) were mainly stabilized through van der Waals, π–alkyl interactions, and carbon hydrogen bonds with the catalytic residues HIS57 and SER195 and the active-site residues such as LEU99, VAL213, SER214, PHE215, and CYS220. Epicatechin (Figure 3d), with a binding energy of −7.3 kcal/mol, formed conventional hydrogen bonds with SER190, ASN192, and CYS191, suggesting stable engagement at the active site. Piperine (Figure 3e) exhibited a binding energy of −6.6 kcal/mol, forming conventional and carbon hydrogen bonds with SER69, SER195, and ASN192, and interacted hydrophobically with residues such as HIS57, LEU99, and CYS191. Procyanidin B1 (Figure 3f) showed the strongest binding affinity (−7.7 kcal/mol), forming multiple hydrogen bonds with ASN192, SER217, GLY216, SER217, and SER217A. In addition, the oxygen atom of this compound could form sulfur-X interaction with the CYS220 residue. These detailed docking results highlight the potential of these compounds to inhibit elastase by engaging key catalytic residues, thereby contributing to anti-wrinkle and skin-firming effects.

Docking simulations with collagenase revealed multiple stabilizing interactions between phytochemicals in the MKDK formula and the enzyme's active site (Figure 4). Alpha-cyperone (Figure 4b) showed the weakest binding energy (−5.8 kcal/mol), forming hydrophobic and π interactions with HIS523, GLU524, HIS527, and GLU555. D-tetrahydropalmatine (Figure 4c) bound with moderate affinity (−6.6 kcal/mol), primarily via π–alkyl interac-

tions and van der Waals forces with residues such as PHE515, LEU520, HIS523, GLU555, and PHE606. In addition, its aromatic moiety formed π–anion interactions with GLU559. Epicatechin (Figure 4d), also at −6.6 kcal/mol, formed multiple hydrogen bonds with GLY493, GLY494, GLU524, and GLU555, as well as π–π stacking and π–anion interactions with HIS527 and GLU555, respectively, suggesting a strong and stable interaction. Piperine (Figure 4e) exhibited a binding energy of −6.7 kcal/mol, engaging residues such as ILE497, GLU498, HIS527, TRP539, and GLU555 through π–alkyl, carbon hydrogen bonding, and hydrophobic contacts. Procyanidin B1 (Figure 4f) demonstrated the highest binding affinity (−7.7 kcal/mol), forming several hydrophobic contacts, as well as a dense hydrogen bonding network with the GLY494, TYR506, GLU524, GLU555, GLU559, TYR579 residues, indicating strong stabilization within the collagenase's active-site pocket. These findings provide mechanistic support for the inhibitory activity of the formula against collagenase, a key enzyme involved in collagen degradation and wrinkle formation.

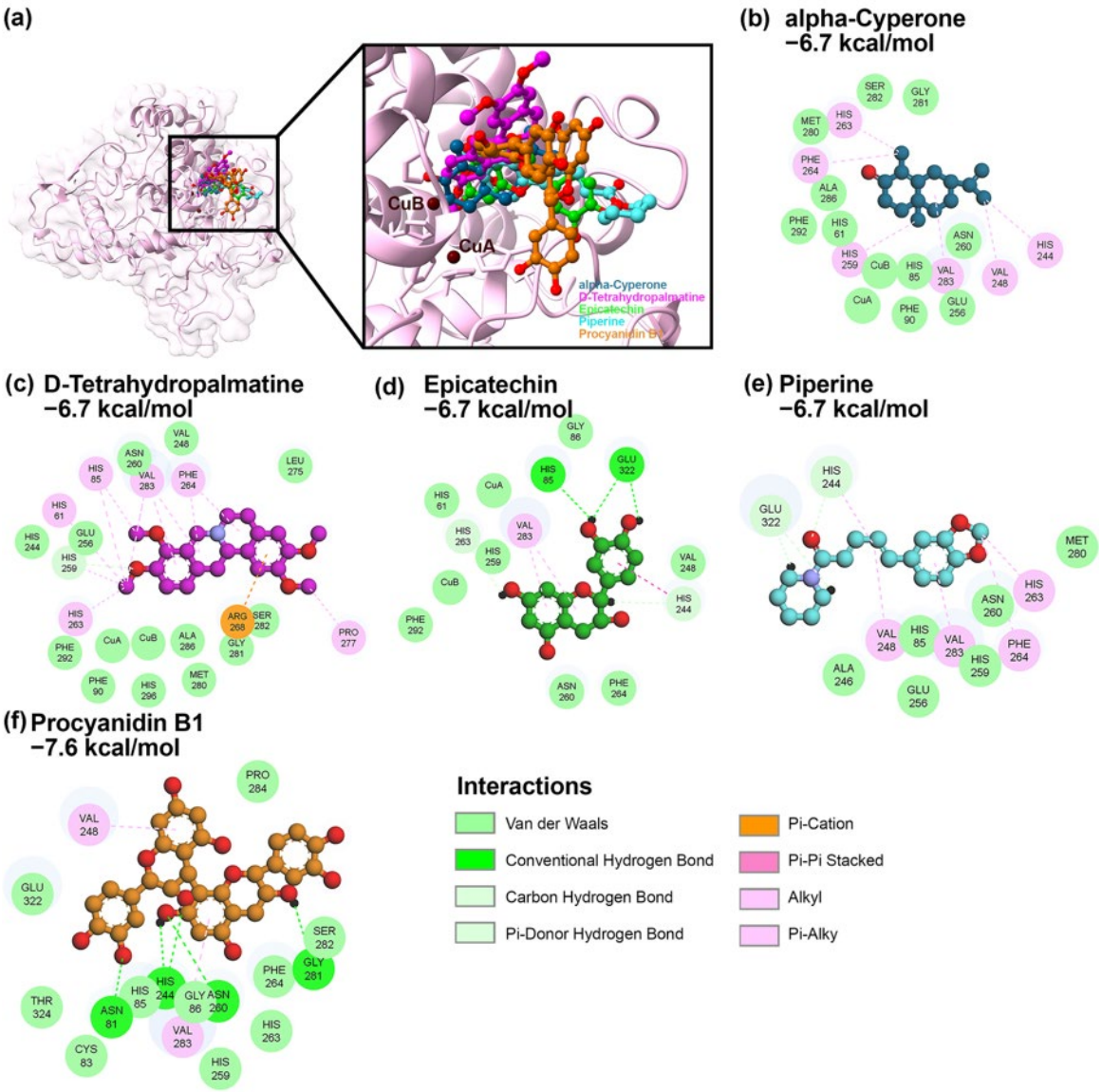


Figure 2. Superimposed docked structure of the key bioactive compounds from the MKDK formula against tyrosinase. (**a**) Superimposed binding poses of the selected bioactive compounds within the active site of tyrosinase, with an enlarged view of the docking pocket showing interactions near the catalytic copper ions (CuA and CuB). 2D interaction profile of (**b**) alpha-cyperone, (**c**) D-tetrahydropalmatine, (**d**) epicatechin, (**e**) piperine, and (**f**) procyanidin B1 in complexes with tyrosinase.

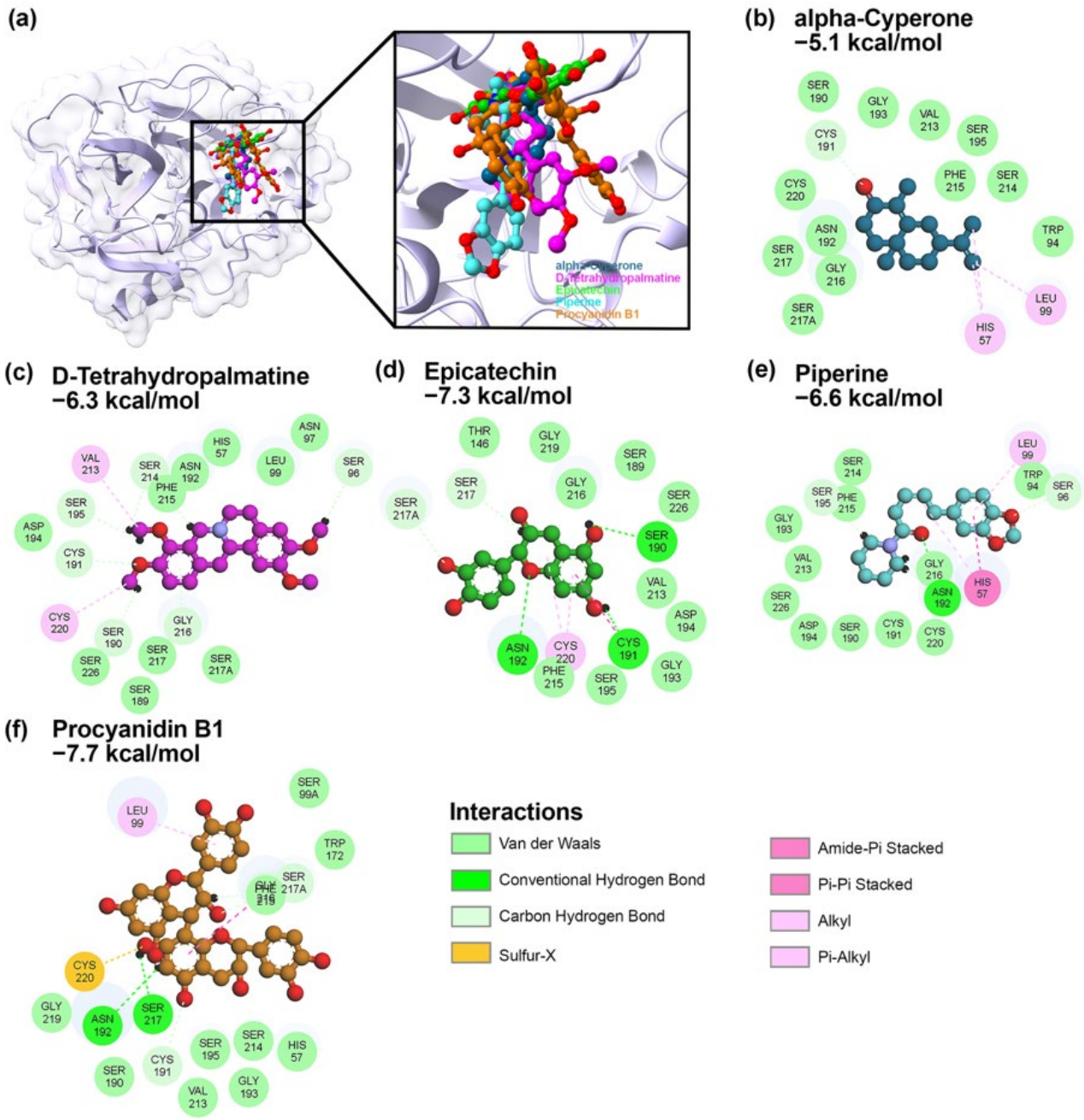


Figure 3. Superimposed docked structure of the key bioactive compounds from the MKDK formula against elastase. (**a**) Superimposed docking poses of the selected phytochemicals within the active site of elastase, together with an enlarged view of the binding pocket. 2D interaction profile of (**b**) alpha-cyperone, (**c**) D-tetrahydropalmatine, (**d**) epicatechin, (**e**) piperine, and (**f**) procyanidin B1 in complexes with elastase.

The molecular docking analysis of selected compounds with hyaluronidase showed differential binding affinities and interactions (Figure 5). Alpha-cyperone (Figure 5b) displayed the weakest binding energy (−6.5 kcal/mol), engaging in hydrophobic interactions primarily with residues such as TYR75, TYR202, TRP321. Moreover, its carbonyl group formed hydrogen bonds with the catalytic TYR247 residue. D-tetrahydropalmatine (Figure 5c) bound with moderate affinity (−7.2 kcal/mol), forming several π interactions with ILE73, ASP129, GLU131, TYR247, TRP321. Moreover, this compound could form hydrogen bonds with the ASN37 and TYR75 residues. Epicatechin (Figure 5d) exhibited a binding energy of −6.9 kcal/mol and formed multiple π interactions with ASP129,

TYR202, TRP321. Moreover, this compound could form hydrogen bonds with GLU131 and TYR247, stabilizing its conformation within the binding pocket. Piperine (Figure 5e), with a higher binding affinity (−7.9 kcal/mol), demonstrated π–anion, hydrogen bond, and alkyl interactions with ILE73, VAL127, ASP129, GLU131, TYR202, TYR247, TYR286, ASP292, and TRP321, suggesting effective anchoring at the enzyme's active site. Procyanidin B1 (Figure 5f) showed the strongest binding (−8.2 kcal/mol), engaging in extensive hydrogen bonding, π interactions, and hydrophobic interactions with multiple residues including SER76, ASP129, GLU131, ALA132, TRP321, and TRP324. These interactions likely contribute to its potent hyaluronidase inhibitory activity, relevant for skin hydration and elasticity preservation.

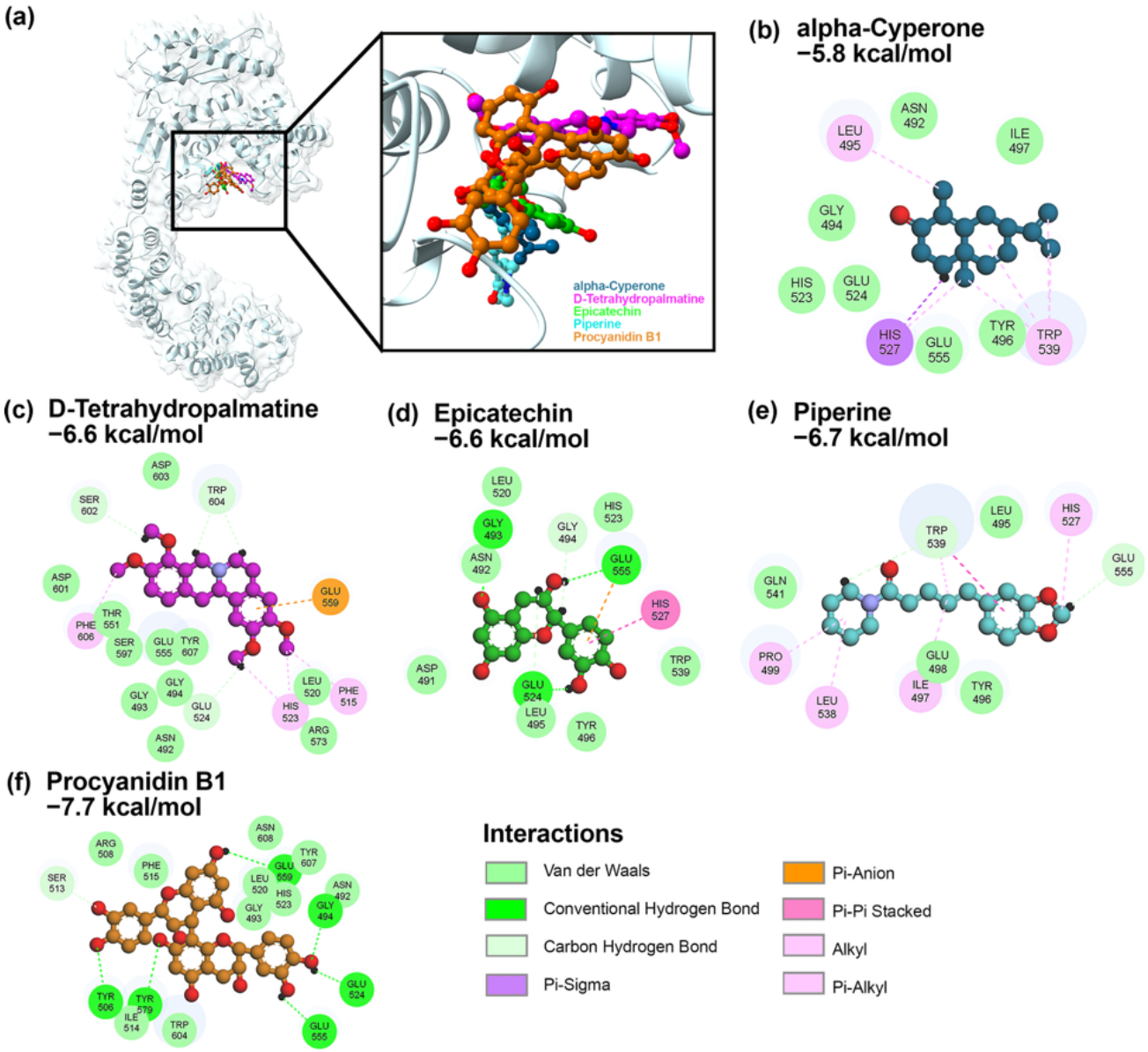


Figure 4. Superimposed docked structure of the key bioactive compounds from the MKDK formula against collagenase. (**a**) Superimposed docking poses of the selected phytochemicals within the active site of collagenase, together with a magnified view of the binding pocket. 2D interaction profile of (**b**) alpha-cyperone, (**c**) D-tetrahydropalmatine, (**d**) epicatechin, (**e**) piperine, and (**f**) procyanidin B1 in complexes with collagenase.

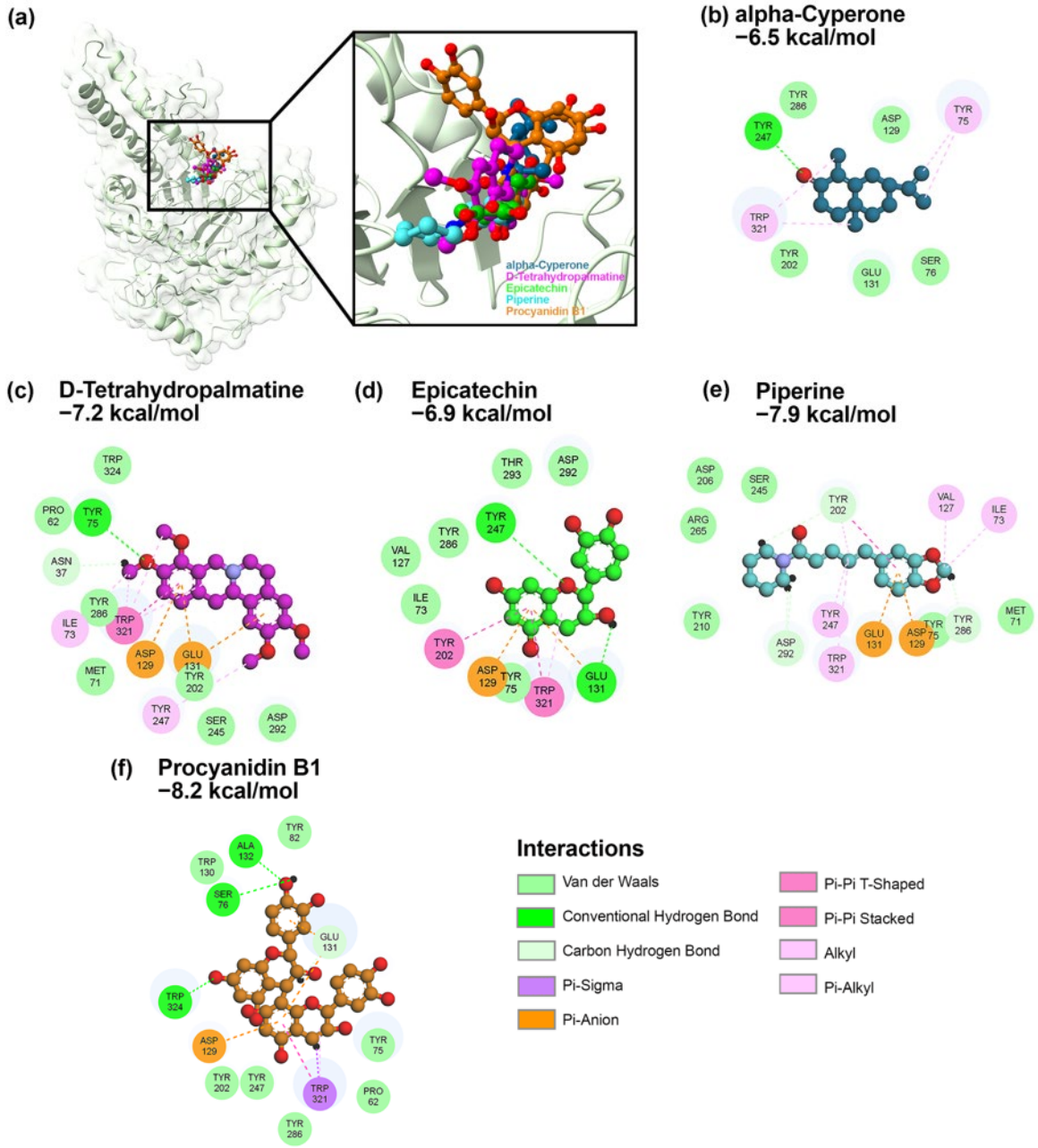


Figure 5. Superimposed docked structure of the key bioactive compounds from the MKDK formula against hyaluronidase. (**a**) Superimposed docking poses of the selected phytochemicals within the active site of hyaluronidase, together with a magnified view of the binding pocket. 2D interaction profile of (**b**) alpha-cyperone, (**c**) D-tetrahydropalmatine, (**d**) epicatechin, (**e**) piperine, and (**f**) procyanidin B1 in complexes with hyaluronidase.

4. Discussion

This study presents evidence for the skin anti-aging efficacy of the traditional Thai herbal formula Mai-Kae-Den-Klong (MKDK), utilizing a comprehensive methodology that involves phytochemical profiling, network pharmacology, molecular docking, and enzyme-based bioassays. The results highlight the formula's multi-target efficacy against critical biochemical and cellular processes related to skin aging, such as oxidative stress, extracellular matrix disintegration, and pigmentation.

LC-MS profiling identified an extensive variety of bioactive phytochemicals, particularly alpha-cyperone, D-tetrahydropalmatine, procyanidin B1, epicatechin, and piperine. The presence of these compounds may partially explain the observed antioxidant activity

and enzyme inhibitory effects of the extract, including the inhibition of matrix-degrading enzymes and tyrosinase, which are relevant to skin-aging processes.

Alpha-cyperone, a sesquiterpenoid component of *C. rotundus*, exhibits antioxidant potential primarily through the modulation of intracellular redox signaling rather than direct free radical scavenging. In in vivo studies using a chronic kidney disease (CKD) model, alpha-cyperone significantly reduced oxidative stress markers, such as reactive oxygen species (ROS), superoxide anion, and 8-hydroxy-2′-deoxyguanosine (8-OHdG), and restored the activity of the antioxidant enzyme superoxide dismutase (SOD) [46]. Mechanistically, it acts by activating the Akt/Nrf2/HO-1 pathway, thereby upregulating endogenous antioxidant defense systems and inhibiting the NF-κB pathway, which suppresses inflammation-induced ROS production [47]. Additionally, alpha-cyperone has been reported to protect neuronal and hepatic cells by stabilizing mitochondrial function and preventing lipid peroxidation [48]. These integrated pathways indicate that alpha-cyperone supports the antioxidant activity of the MKDK formula by enhancing the skin's intrinsic antioxidant response and mitigating oxidative stress associated with skin aging. In molecular docking tests, it had comparatively low affinities for elastase (−5.1 kcal/mol), collagenase (−5.8 kcal/mol), and hyaluronidase (−6.5 kcal/mol), indicating a potential function in enzyme inhibition. Binding to tyrosinase (−6.7 kcal/mol) through hydrophobic interactions with HIS263 and PHE264 may result in moderate anti-pigmentation effects [49].

Epicatechin, a flavonoid with high abundance in the extract, has demonstrated promising multifunctional properties relevant to skin anti-aging. Its antioxidant activity is primarily attributed to the presence of multiple hydroxyl groups capable of neutralizing ROS through electron donation. In UVB-induced BJ fibroblast models, epicatechin significantly enhanced endogenous antioxidant responses by upregulating GPX-1 gene expression and increasing melatonin levels while simultaneously reducing levels of oxidative DNA damage marker 8-OHdG, cyclooxygenase-2 (COX-2), and ROS-associated apoptosis [50]. Additionally, epicatechin exhibits inhibitory effects against enzymes responsible for extracellular matrix degradation. It significantly downregulated MMP-1 expression, an enzyme responsible for collagen breakdown, while increasing the expression of COL1A1, FGF-2, and elastin proteins, thereby supporting collagen integrity and skin elasticity [50]. Catechin and epicatechin, which are prominent tannin compounds found abundantly in green tea and other plant sources such as Vigna angularis, have been reported to exhibit strong tyrosinase inhibitory activity [51,52]. Docking analysis revealed robust interactions with all enzymes tested, elastase (−7.3 kcal/mol), collagenase (−6.6 kcal/mol), and hyaluronidase (−6.9 kcal/mol), indicating strong inhibition of extracellular matrix degradation. Tyrosinase binding at −6.7 kcal/mol involved hydrogen bonding with HIS244 and GLU322, supporting its contribution to anti-melanogenesis effects. As the most potent bioactive identified, procyanidin B1 exhibited the strongest antioxidant potential due to its dimeric polyphenolic structure and high peak intensity in LC-MS data.

Proanthocyanidins derived from grape seeds have been shown to suppress oxidative stress induced by UV exposure and to inhibit the activation of MAPK and NF-κB signaling pathways in human epidermal keratinocytes [53]. *Pinus densiflora* extract (PDE), which is rich in proanthocyanidins, has demonstrated multifaceted skin-protective effects relevant to anti-aging. It has been reported to inhibit tyrosinase activity and L-DOPA oxidation, indicating potential for pigmentation control [54]. Moreover, PDE has shown strong anti-photoaging activity by mitigating UVB-induced oxidative stress, reducing elastase activity, and downregulating the expression of matrix metalloproteinases (MMP-1, -2, -3, and -9) in human dermal fibroblasts. These effects are accompanied by the restoration of collagen synthesis through the modulation of Smad signaling, upregulating Smad3 while suppressing Smad7, and the inhibition of AP-1 transcription factors such as c-Jun and c-Fos, which are

key mediators of MMP induction [55]. This compound showed the highest binding affinity across all target enzymes: −7.7 kcal/mol for elastase and collagenase, and −8.2 kcal/mol for hyaluronidase. For tyrosinase, a docking score of −7.6 kcal/mol was observed, with extensive hydrogen bonding and van der Waals interactions. These findings highlight its central role in both enzymatic and oxidative aspects of skin aging prevention. Piperine, a bioactive alkaloid from *Piper nigrum*, has been shown to protect keratinocytes from UVB-induced damage by enhancing cell viability and reducing intracellular ROS, nitric oxide, and nitrite levels. It also suppressed the p38 and JNK signaling pathways, leading to decreased expression of inflammatory mediators (iNOS, COX-2) and pro-inflammatory cytokines (IL-6, IL-8) [56].

Piperine has been identified as a potent natural tyrosinase inhibitor, demonstrating significant anti-melanogenic activity without cytotoxic effects [57]. In this study, piperine demonstrated moderate binding affinities to elastase (−6.6 kcal/mol), collagenase (−6.7 kcal/mol), and hyaluronidase (−7.9 kcal/mol), reflecting broad but non-specific inhibitory action. Tyrosinase docking (−6.7 kcal/mol) revealed π–alkyl and van der Waals interactions with active-site residues. The multi-target interactions of this compound may contribute to the observed anti-aging properties of the formula, particularly through mechanisms associated with wrinkle prevention and pigmentation regulation.

Tetrahydropalmatine (THP) has demonstrated antioxidant activity by reducing oxidative stress and lipid peroxidation in a hyperlipidemic animal model [58]. Despite its lower abundance, THP contributed to skin-aging enzyme inhibition with docking energies of −6.3 kcal/mol (elastase), −6.6 kcal/mol (collagenase), and −7.2 kcal/mol (hyaluronidase). It also showed tyrosinase inhibition (−6.7 kcal/mol), supporting its potential involvement in anti-pigmentation effects. To the best of our knowledge, there are currently no published reports on the anti-tyrosinase or skin anti-aging effects of THP, making these findings novel and worthy of further investigation.

Together, the results of this study, supported by published evidence, suggest that the bioactive phytochemicals identified in the MKDK extract, particularly alpha-cyperone, epicatechin, procyanidin B1, piperine, and tetrahydropalmatine, may collectively contribute to skin anti-aging effects. The integration of LC-MS profiling, molecular docking, and literature-based biological activities highlights their potential in mitigating oxidative stress, preserving dermal structure, and regulating melanogenesis. These findings together support the therapeutic potential of this traditional herbal formula for holistic skin anti-aging applications.

Through network pharmacology, the predicted targets of major phytochemicals were enriched in aging-related pathways such as FoxO signaling, focal adhesion, chemokine signaling, and metabolic regulation. The FoxO pathway, in particular, is a critical modulator of longevity and stress resistance by influencing apoptosis, antioxidant enzyme expression, and DNA repair [59,60]. This supports the hypothesis that the formula modulates fundamental biological processes involved in intrinsic aging and cellular homeostasis.

The collective activity of MKDK may arise from the combined contributions of its bioactive constituents, consistent with the polyherbal philosophy of Thai traditional medicine. While many studies focus on isolated compounds, this research affirms the therapeutic merit of traditional multi-herb formulas by demonstrating both broad-spectrum bioactivities and predicted pathway modulation at the systems level. The study advances the scientific understanding of how traditional formulas can exert anti-aging effects through complementary mechanisms, antioxidant protection, enzymatic inhibition, and pathway regulation.

Despite the promising results, several limitations should be acknowledged. First, the antioxidant, tyrosinase, elastase, collagenase, and hyaluronidase assays employed in this study are widely used for the preliminary screening of anti-aging activity; however, they are insufficient to confirm comprehensive anti-aging efficacy. Important biological

processes associated with skin aging, including collagen synthesis, cell-based responses, antiglycation activity, cellular senescence markers, dermal penetration, and clinical skin outcomes, were not evaluated. Second, the enzyme-based bioassays and computational analyses do not fully replicate the complex physiology of human skin. Third, the network pharmacology predictions were derived from publicly available databases and may not capture all relevant biological targets or reflect pharmacokinetic and bioavailability constraints. Therefore, future studies should include mechanistic investigations using relevant skin-cell models, dermal penetration assessments, formulation optimization, and safety evaluations. In addition, well-designed clinical studies are required to validate the efficacy and safety of MKDK for cosmetic applications. Future computational studies may also incorporate docking validation approaches, such as redocking of co-crystallized ligands or comparison with known inhibitors, to further strengthen the reliability of the predicted ligand–target interactions. Furthermore, bioavailability studies of key phytochemicals, such as procyanidin B1 and piperine, would be valuable for supporting the development of topical or oral cosmeceutical formulations.

5. Conclusions

The findings suggest that MKDK may represent a promising source of bioactive compounds for cosmetic anti-aging applications. LC-MS metabolite profiling identified a chemically diverse extract abundant in flavonoids, alkaloids, and terpenoids, which are recognized for their antioxidant and anti-aging properties. Network pharmacology analysis suggests that these phytochemicals may influence important signaling pathways associated with oxidative stress response, inflammation, and extracellular matrix homeostasis, especially via the FoxO signaling pathway. Molecular docking simulations verified these findings by demonstrating substantial binding affinities of significant constituents, including procyanidin B1 and epicatechin, to essential enzymes associated with skin aging. The extract demonstrated significant antioxidant activity and moderate inhibitory effects on elastase, collagenase, hyaluronidase, and tyrosinase in enzyme-based bioassays. The results collectively demonstrate the formula's potential as a natural cosmeceutical agent for preventing or reducing the effects of skin aging. Further studies involving clinical evaluation and formulation development are necessary to explore its therapeutic application in dermatology and skincare.

Supplementary Materials: The following supporting information can be downloaded at: https://www.mdpi.com/article/10.3390/cosmetics13030158/s1, Table S1. LC–MS-identified metabolites detected in the MKDK extract.

Author Contributions: Conceptualization, T.C., N.W. and A.D.; methodology, T.C. and A.D.; software, P.M. and K.S.W.; validation, T.C., N.W. and A.D.; formal analysis, S.S. and K.P.; investigation, T.C., N.W., K.P., S.C. and S.S.; resources, A.D.; data curation, P.M. and A.D.; writing—original draft preparation, T.C., N.W. and K.P.; writing—review and editing, A.D. and S.P.B.; visualization, P.M. and K.S.W.; supervision, A.D. and S.P.B.; project administration, A.D.; funding acquisition, T.C. and A.D. All authors have read and agreed to the published version of the manuscript.

Funding: This research was funded by Thailand Science Research and Innovation (TSRI) through Ubon Ratchathani Rajabhat University in 2025.

Institutional Review Board Statement: Not applicable.

Informed Consent Statement: Not applicable.

Data Availability Statement: The raw data supporting the conclusions of this article will be made available by the authors on request.

Acknowledgments: The authors gratefully acknowledge the Faculty of Thai Traditional and Alternative Medicine, Ubon Ratchathani Rajabhat University (UBRU), Thailand, for research facility support.

During the preparation of this manuscript, the authors used ChatGPT (OpenAI, GPT-5.5) to assist with language editing and grammar correction. The authors have reviewed and edited the output and take full responsibility for the content of this publication.

Conflicts of Interest: The authors declare that they have no known competing financial interests or personal relationships that could have appeared to influence the work reported in this paper.

Abbreviations

The following abbreviations are used in this manuscript:

ABTS	2,2′-Azino-bis(3-ethylbenzothiazoline-6-sulfonic acid)
ECM	Extracellular matrix
CKD	Chronic kidney disease
COX-2	Cyclooxygenase-2
DPPH	2,2-Diphenyl-1-picrylhydrazyl
FDR	False discovery rate
FALGPA	N-[3-(2-furyl)acryloyl]-Leu-Gly-Pro-Ala
GO	Gene Ontology
LC-MS	Liquid chromatography mass spectrometry
ROS	Reactive oxygen species
SANA	N-succinyl-Ala-Ala-Pro-p-nitroanilide
SOD	Superoxide dismutase
THP	Tetrahydropalmatine

References

1. George, J.; Sneed, K.; Pathak, Y. The Skin Aging Process and Anti-Aging Strategies. *Biomed. J. Sci. Tech. Res.* **2022**, *42*, 33377–33386. [CrossRef]
2. Furman, D.; Auwerx, J.; Bulteau, A.-L.; Church, G.; Couturaud, V.; Crabbe, L.; Davies, K.J.A.; Decottignies, A.; Gladyshev, V.N.; Kennedy, B.K.; et al. Skin Health and Biological Aging. *Nat. Aging* **2025**, *5*, 1195–1206. [CrossRef] [PubMed]
3. Hussein, R.S.; Bin Dayel, S.; Abahussein, O.; El-Sherbiny, A.A. Influences on Skin and Intrinsic Aging: Biological, Environmental, and Therapeutic Insights. *J. Cosmet. Dermatol.* **2025**, *24*, e16688. [CrossRef] [PubMed]
4. Nan, L.; Guo, P.; Hui, W.; Xia, F.; Yi, C. Recent Advances in Dermal Fibroblast Senescence and Skin Aging: Unraveling Mechanisms and Pioneering Therapeutic Strategies. *Front. Pharmacol.* **2025**, *16*, 1592596. [CrossRef] [PubMed]
5. Wang, Y.; Jiang, R.; Xiong, B.; Zhu, J.; Sang, J.; Li, H.; Chen, C.; Xu, Z.; Zhang, W.; Chen, Y.; et al. Clinical Investigation of Tyrosinase Inhibitors: Past, Present, and Future. *Drug Dev. Res.* **2025**, *86*, e70113. [CrossRef] [PubMed]
6. Tomas, M.; Günal-Köroğlu, D.; Kamiloglu, S.; Ozdal, T.; Capanoglu, E. The State of the Art in Anti-Aging: Plant-Based Phytochemicals for Skin Care. *Immun. Ageing* **2025**, *22*, 5. [CrossRef] [PubMed]
7. Saini, V.; Deswal, G.; Grewal, A.S.; Sharma, A.; Guarve, K. Natural Anti-Aging Strategies: Mechanisms and Role of Phytoextracts in Combating Skin Aging. *Arch. Dermatol. Res.* **2025**, *317*, 312. [CrossRef] [PubMed]
8. Bouissane, L.; Elfardi, Y.; Khatib, S.; Fatimi, A.; Pereira, C.; Cruz-Martins, N. Medicinal Plants and Their Derivatives for Skin and Hair: A Mediterranean Perspective of Women Care. *Arch. Dermatol. Res.* **2025**, *317*, 710. [CrossRef] [PubMed]
9. Abedelmaksoud, T.G.; Younis, M.I.; Altemimi, A.B.; Tlay, R.H.; Ali Hassan, N. Bioactive Compounds of Plant-Based Food: Extraction, Isolation, Identification, Characteristics, and Emerging Applications. *Food Sci. Nutr.* **2025**, *13*, e70351. [CrossRef] [PubMed]
10. Manful, M.E.; Ahmed, L.; Barry-Ryan, C. Cosmetic Formulations from Natural Sources: Safety Considerations and Legislative Frameworks in the European Union. *Cosmetics* **2024**, *11*, 72. [CrossRef]
11. Wang, L.; Zuo, X.; Ouyang, Z.; Qiao, P.; Wang, F. A Systematic Review of Antiaging Effects of 23 Traditional Chinese Medicines. *Evid. Based Complement. Altern. Med.* **2021**, *2021*, 5591573. [CrossRef] [PubMed]
12. Bolat, E.; Karagöz, Z.; Alves, J.L.D.B.; Neto, J.P.R.C.; Witkowska, A.M.; El-Seedi, H.; Lombardo, M.; Karav, S. The Potential Applications of Natural Colostrum in Skin Health. *Cosmetics* **2024**, *11*, 197. [CrossRef]
13. Rybczyńska-Tkaczyk, K.; Grenda, A.; Jakubczyk, A.; Kiersnowska, K.; Bik-Małodzińska, M. Natural Compounds with Antimicrobial Properties in Cosmetics. *Pathogens* **2023**, *12*, 320. [CrossRef] [PubMed]
14. Silletta, A.; Mancuso, A.; d'Avanzo, N.; Cristiano, M.C.; Paolino, D. Antimicrobial Compounds from Food Waste in Cosmetics. *Cosmetics* **2024**, *11*, 151. [CrossRef]
15. Fernandes, A.; Rodrigues, P.M.; Pintado, M.; Tavaria, F.K. A Systematic Review of Natural Products for Skin Applications: Targeting Inflammation, Wound Healing, and Photo-Aging. *Phytomedicine* **2023**, *115*, 154824. [CrossRef] [PubMed]

16. Costa, E.F.; Magalhães, W.V.; Di Stasi, L.C. Recent Advances in Herbal-Derived Products with Skin Anti-Aging Properties and Cosmetic Applications. *Molecules* **2022**, *27*, 7518. [CrossRef] [PubMed]
17. Sivakrishnan, S.; Muthu, A.K. In-vitro Free Radical Scavenging Activity of Aerial Aarts of Ethanolic Extract of *Albizia procera* (family: Mimosoideae). *Int. J. Pharm. Pharm. Sci.* **2013**, *5*, 352–354.
18. Pramanik, A.; Maheshwari, S.; Acharya, N. Medicinal Plants, Antioxidant Potential, and Applications to Aging. In *Role of Herbal Medicines*; Dhara, A.K., Mandal, S.C., Eds.; Springer Nature: Singapore, 2023; pp. 403–413. ISBN 978-981-99-7702-4.
19. Wongchum, N.; Dechakhamphu, A. Extract from the Stem of *Tinospora crispa* (L.) Hook. f. & Thomson Extends Life Span and Decreases Stress-Induced Mortality in *Drosophila melanogaster*. *Pharm. Sci. Asia* **2022**, *49*, 86–97. [CrossRef]
20. Wongchum, N.; Dechakhamphu, A.; Ma-ding, A.; Khamphaeng, T.; Pinlaor, S.; Pinmongkhonkul, S.; Tanomtong, A. The Effects of *Cyperus rotundus* L. Extracts on the Longevity of *Drosophila melanogaster*. *S. Afr. J. Bot.* **2022**, *148*, 218–227. [CrossRef]
21. Phongsuwichetsak, C.; Suksrichavalit, T.; Chatupheeraphat, C.; Eiamphungporn, W.; Yainoy, S.; Yamkamon, V. *Diospyros rhodocalyx* Kurz Induces Mitochondrial-Mediated Apoptosis *via* BAX, Bcl-2, and Caspase-3 Pathways in LNCaP Human Prostate Cancer Cell Line. *PeerJ* **2024**, *12*, e17637. [CrossRef] [PubMed]
22. Somwong, P.; Theanphong, O. Quantitative Analysis of Triterpene Lupeol and Anti-Inflammatory Potential of the Extracts of Traditional Pain-Relieving Medicinal Plants *Derris scandens*, *Albizia procera*, and *Diospyros rhodocalyx*. *J. Adv. Pharm. Technol. Res.* **2021**, *12*, 147–151. [CrossRef] [PubMed]
23. Thengyai, S.; Thiantongin, P.; Sontimuang, C.; Ovatlarnporn, C.; Puttarak, P. α-Glucosidase and α-Amylase Inhibitory Activities of Medicinal Plants in Thai Antidiabetic Recipes and Bioactive Compounds from *Vitex glabrata* R. Br. Stem Bark. *J. Herb. Med.* **2020**, *19*, 100302. [CrossRef]
24. Minsakorn, S.; Watthanadirek, A.; Poolsawat, N.; Puttarak, P.; Chawengkirttikul, R.; Anuracpreeda, P. The Anthelmintic Potentials of Medicinal Plant Extracts and an Isolated Compound (Rutin, C27H30O16) from *Terminalia catappa* L. against Gastrothylax Crumenifer. *Vet. Parasitol.* **2021**, *291*, 109385. [CrossRef] [PubMed]
25. Kraithep, S.; Oungbho, K.; Tewtrakul, S. Anti-Allergic Activity of Thai Medicinal Plants Used in Longevity Formulation. *Songklanakarin J. Sci. Technol.* **2008**, *30*, 624–625.
26. Zou, R.; Zhou, Y.; Lu, Y.; Zhao, Y.; Zhang, N.; Liu, J.; Zhang, Y.; Fu, Y. Preparation, Pungency and Bioactivity Transduction of Piperine from Black Pepper (*Piper nigrum* L.): A Comprehensive Review. *Food Chem.* **2024**, *456*, 139980. [CrossRef] [PubMed]
27. Wongchum, N.; Dechakhamphu, A.; Panya, P.; Pinlaor, S.; Pinmongkhonkul, S.; Tanomtong, A. Hydroethanolic *Cyperus rotundus* L. Extract Exhibits Anti-Obesity Property and Increases Lifespan Expectancy in *Drosophila melanogaster* Fed a High-Fat Diet. *J. Herbmed Pharmacol.* **2022**, *11*, 296–304. [CrossRef]
28. Chaudhary, A.; Das, R.; Mehta, K.; Mehta, D.K. Indian Herb *Tinospora cordifolia* and *Tinospora* Species: Phytochemical and Therapeutic Application. *Heliyon* **2024**, *10*, e31229. [CrossRef] [PubMed]
29. Chamariya, R.; Raheja, R.; Suvarna, V.; Bhandare, R. A Critical Review on Phytopharmacology, Spectral and Computational Analysis of Phytoconstituents from *Streblus asper* Lour. *Phytomed. Plus* **2022**, *2*, 100177. [CrossRef]
30. Joshi, C.P.; Baldi, A.; Kumar, N.; Pradhan, J. Harnessing Network Pharmacology in Drug Discovery: An Integrated Approach. *Naunyn-Schmiedeberg's Arch. Pharmacol.* **2025**, *398*, 4689–4703. [CrossRef]
31. Zhai, Y.; Liu, L.; Zhang, F.; Chen, X.; Wang, H.; Zhou, J.; Chai, K.; Liu, J.; Lei, H.; Lu, P.; et al. Network Pharmacology: A Crucial Approach in Traditional Chinese Medicine Research. *Chin. Med.* **2025**, *20*, 8. [CrossRef] [PubMed]
32. Sahu, M.K.; Nayak, A.K.; Hailemeskel, B.; Eyupoglu, O.E. Exploring Recent Updates on Molecular Docking: Types, Method, Application, Limitation & Future Prospects. *Int. J. Pharm. Res. Allied Sci.* **2024**, *13*, 24–40. [CrossRef]
33. Muhammed, M.T.; Aki-Yalcin, E. Molecular Docking: Principles, Advances, and Its Applications in Drug Discovery. *Lett. Drug Des. Discov.* **2024**, *21*, 480–495. [CrossRef]
34. Bisht, A.; Tewari, D.; Kumar, S.; Chandra, S. Network Pharmacology, Molecular Docking, and Molecular Dynamics Simulation to Elucidate the Mechanism of Anti-Aging Action of *Tinospora cordifolia*. *Mol. Divers.* **2024**, *28*, 1743–1763. [CrossRef] [PubMed]
35. Paggi, J.M.; Pandit, A.; Dror, R.O. The Art and Science of Molecular Docking. *Annu. Rev. Biochem.* **2024**, *93*, 389–410. [CrossRef] [PubMed]
36. Sarkar, J.; Singh, R.; Chandel, S. Understanding LC/MS-Based Metabolomics: A Detailed Reference for Natural Product Analysis. *Proteom. Clin. Appl.* **2025**, *19*, e202400048. [CrossRef]
37. Dechakhamphu, A.; Wongchum, N.; Singthong, P.; Chumroenphat, T.; Tanomtong, A.; Siriamornpun, S. Exploring the Functional Supplement Potential of the Thai Herbal Formula Tri-Ka-Tuk via Metabolomic and Proteomic Profiling in *Drosophila*. *Food Biosci.* **2025**, *73*, 107637. [CrossRef]
38. Daina, A.; Michielin, O.; Zoete, V. SwissTargetPrediction: Updated Data and New Features for Efficient Prediction of Protein Targets of Small Molecules. *Nucleic Acids Res.* **2019**, *47*, W357–W364. [CrossRef] [PubMed]
39. Kanehisa, M.; Furumichi, M.; Sato, Y.; Ishiguro-Watanabe, M.; Tanabe, M. KEGG: Integrating Viruses and Cellular Organisms. *Nucleic Acids Res.* **2021**, *49*, D545–D551. [CrossRef] [PubMed]

40. Ge, S.X.; Jung, D.; Yao, R. ShinyGO: A Graphical Gene-Set Enrichment Tool for Animals and Plants. *Bioinformatics* **2020**, *36*, 2628–2629. [CrossRef] [PubMed]
41. Luo, W.; Brouwer, C. Pathview: An R/Bioconductor Package for Pathway-Based Data Integration and Visualization. *Bioinformatics* **2013**, *29*, 1830–1831. [CrossRef] [PubMed]
42. Chumroenphat, T.; Wongchum, N.; Thangthong, C.; Wongsrikaew, D.; Dechakhamphu, A. Developmental Stage-Dependent Phytochemical Composition and Bioactivities of *Shorea roxburghii* G. Don Edible Flowers with Potential for Nutraceutical and Functional Food Applications. *J. Food Meas. Charact.* **2025**, *19*, 6366–6383. [CrossRef]
43. Angelis, A.; Mavros, P.; Nikolaou, P.E.; Mitakou, S.; Halabalaki, M.; Skaltsounis, L. Phytochemical Analysis of Olive Flowers' Hydroalcoholic Extract and in Vitro Evaluation of Tyrosinase, Elastase and Collagenase Inhibition Activity. *Fitoterapia* **2020**, *143*, 104602. [CrossRef] [PubMed]
44. Lee, K.-K.; Kim, J.-H.; Cho, J.-J.; Choi, J.D. Inhibitory Effects of 150 Plant Extracts on Elastase Activity, and Their Anti-inflammatory Effects. *Int. J. Cosmet. Sci.* **1999**, *21*, 71–82. [CrossRef] [PubMed]
45. Abdelfattah, M.A.O.; Dmirieh, M.; Ben Bakrim, W.; Mouhtady, O.; Ghareeb, M.A.; Wink, M.; Sobeh, M. Antioxidant and Anti-Aging Effects of *Warburgia salutaris* Bark Aqueous Extract: Evidences from in Silico, in Vitro and in Vivo Studies. *J. Ethnopharmacol.* **2022**, *292*, 115187. [CrossRef] [PubMed]
46. Chen, W.; Mao, J.; Li, C.; Ke, J. Alpha-Cyperone Ameliorates Renal Fibrosis and Inflammation in Mice with Chronic Kidney Disease *via* NF-κB and Akt/Nrf2/HO-1 Pathways. *Immunopharmacol. Immunotoxicol.* **2025**, *47*, 460–470. [CrossRef] [PubMed]
47. Huang, B.; Liu, J.; Fu, S.; Zhang, Y.; Li, Y.; He, D.; Ran, X.; Yan, X.; Du, J.; Meng, T.; et al. α-Cyperone Attenuates H_2O_2-Induced Oxidative Stress and Apoptosis in SH-SY5Y Cells via Activation of Nrf2. *Front. Pharmacol.* **2020**, *11*, 281. [CrossRef] [PubMed]
48. Herrera-Calderon, O.; Santiváñez-Acosta, R.; Pari-Olarte, B.; Enciso-Roca, E.; Campos Montes, V.M.; Luis Arroyo Acevedo, J. Anticonvulsant Effect of Ethanolic Extract of *Cyperus articulatus* L. Leaves on Pentylenetetrazol Induced Seizure in Mice. *J. Tradit. Complement. Med.* **2018**, *8*, 95–99. [CrossRef] [PubMed]
49. Nokinsee, D.; Shank, L.; Lee, V.S.; Nimmanpipug, P. Estimation of Inhibitory Effect against Tyrosinase Activity through Homology Modeling and Molecular Docking. *Enzym. Res.* **2015**, *2015*, 262364. [CrossRef] [PubMed]
50. Widowati, W.; Wargasetia, T.L.; Rahardja, F.; Tih, F.; Onggowidjaja, P.; Tjokropranoto, R.; Zahiroh, F.H.; Azis, R.; Priyandoko, D.; Surakusumah, W.; et al. Potential of Epicatechin as Antioxidant and Antiaging in UV-Induced BJ Cells by Regulating COL1A1, FGF-2, GPX-1, and MMP-1 Gene, Protein Levels, and Apoptosis. *PeerJ* **2024**, *12*, e18382. [CrossRef]
51. Chai, W.-M.; Wei, Q.-M.; Deng, W.-L.; Zheng, Y.-L.; Chen, X.-Y.; Huang, Q.; Ou-Yang, C.; Peng, Y.-Y. Anti-Melanogenesis Properties of Condensed Tannins from *Vigna angularis* Seeds with Potent Antioxidant and DNA Damage Protection Activities. *Food Funct.* **2019**, *10*, 99–111. [CrossRef] [PubMed]
52. Liang, Y.; Kang, S.; Deng, L.; Xiang, L.; Zheng, X. Inhibitory Effects of (-)-Epigallocatechin-3-Gallate on Melanogenesis in Ultraviolet A-Induced B16 Murine Melanoma Cell. *Trop. J. Pharm. Res.* **2014**, *13*, 1825. [CrossRef]
53. Mantena, S.K.; Katiyar, S.K. Grape Seed Proanthocyanidins Inhibit UV-Radiation-Induced Oxidative Stress and Activation of MAPK and NF-κB Signaling in Human Epidermal Keratinocytes. *Free Radic. Biol. Med.* **2006**, *40*, 1603–1614. [CrossRef] [PubMed]
54. Hwang, J.H.; Lee, B.M. Inhibitory Effects of Plant Extracts on Tyrosinase, L-DOPA Oxidation, and Melanin Synthesis. *J. Toxicol. Environ. Health A* **2007**, *70*, 393–407. [CrossRef] [PubMed]
55. Jung, H.-Y. *Pinus Densiflora* Extract Protects Human Skin Fibroblasts against UVB-Induced Photoaging by Inhibiting the Expression of MMPs and Increasing Type I Procollagen Expression. *Toxicol. Rep.* **2014**, *1*, 658–666. [CrossRef] [PubMed]
56. Jaisin, Y.; Ratanachamnong, P.; Wongsawatkul, O.; Watthammawut, A.; Malaniyom, K.; Natewong, S. Antioxidant and Anti-Inflammatory Effects of Piperine on UV-B-Irradiated Human HaCaT Keratinocyte Cells. *Life Sci.* **2020**, *263*, 118607. [CrossRef] [PubMed]
57. Khongkarat, P.; Sadangrit, P.; Puthong, S.; Meemongkolkiat, T.; Phuwapraisirisan, P.; Chanchao, C. Anti-Tyrosinase and Anti-Melanogenic Effects of Piperine Isolated from *Piper nigrum* on B16F10 Mouse Melanoma Cells. *Heliyon* **2024**, *10*, e33423. [CrossRef] [PubMed]
58. Ding, K.; Chen, L.; He, J.; Wang, J.; Yu, C.; Wang, H. Tetrahydropalmatine Alleviates Hyperlipidemia by Regulating Lipid Peroxidation, Endoplasmic Reticulum Stress, and Inflammasome Activation by Inhibiting the TLR4-NF-κB Pathway. *Evid. Based Complement. Altern. Med.* **2021**, *2021*, 6614985. [CrossRef] [PubMed]
59. Martins, R.; Lithgow, G.J.; Link, W. Long Live FOXO: Unraveling the Role of FOXO Proteins in Aging and Longevity. *Aging Cell* **2016**, *15*, 196–207. [CrossRef]
60. Perez, F.P.; Moinuddin, S.S.; Ul Ain Shamim, Q.; Joseph, D.J.; Morisaki, J.; Zhou, X. Longevity Pathways: HSF1 and FoxO Pathways, a New Therapeutic Target to Prevent Age-Related Diseases. *Curr. Aging Sci.* **2012**, *5*, 87–95. [CrossRef] [PubMed]

Disclaimer/Publisher's Note: The statements, opinions and data contained in all publications are solely those of the individual author(s) and contributor(s) and not of MDPI and/or the editor(s). MDPI and/or the editor(s) disclaim responsibility for any injury to people or property resulting from any ideas, methods, instructions or products referred to in the content.